Catal Lett (2009) 129:408–415
DOI 10.1007/s10562-008-9811-z

# Textural Properties and Catalytic Applications of ZSM-5 Monolith Foam for Methanol Conversion

**Yun-Jo Lee · Ye-Won Kim · Ki-Won Jun · Nagabhatla Viswanadham · Jong Wook Bae · Hyung-Sang Park**

Received: 12 November 2008 / Accepted: 1 December 2008 / Published online: 9 January 2009


**Abstract** ZSM-5 monolith foam (ZMF) samples with various framework Si/Al ratios have been successfully synthesized by polyurethane foam (PUF) template method and evaluated for their catalytic performance towards methanol to propylene (MTP) reaction. The samples were tested for their textural properties using SEM, XRD, BET surface area, pore volume and $NH_3$-TPD techniques revealing the formation of ZMF exhibiting about 100–300 μm range macro pores created by packed assembly of 5 μm size orthorhombic shaped ZSM-5 crystals. The ZMF samples exhibited effective activity in methanol to olefin conversion, with superior product selectivities at optimum Si/Al ratio of 250. Further, the ZMF catalyst with high macro porosity exhibited superior catalytic activity compared to its pelletized form, especially at higher feed flow rates, that signifies the importance of macro porous structure of ZMF in facilitating the enhanced mass transport for the labile diffusion of light olefins. Reaction temperature also played a vital role in determining product selectivity. At 500 °C, the catalysts exhibited the highest light olefin ($C_2^=$–$C_4^=$) selectivity and above this temperature, formation of $C_5^+$ is prevailed at the cost of $C_2^=$–$C_4^=$ revealing the accelerated occurrence of oligomerization reactions at these conditions. At optimized catalytic properties and reaction conditions, the catalyst exhibited as high as 75% selectivity to $C_2$–$C_4$ olefins, with propylene as major component (~44%).

**Keywords** Zeolite foam · Monolith · Macroporous ZSM-5 · MTP · Methanol · Propylene

## 1 Introduction

Conversion of methanol to light olefins especially propylene is gaining importance due to the significant applications of propylene in the production of various petrochemicals and provides an alternative source to traditional resources such as natural gas, coal and biomass, for the production of gasoline. Zeolites, by virtue of their acidity and selective cracking, have been employed for the MTO reaction [1–6]. The product is generally a mixture of $C_2$–$C_4$ olefins. The well-known Lurgi process operates for the production of propylene from methanol, where gasoline, LPG and fuel gas appear as byproducts that limit the maximization of propylene yields in once-through operation. Hydro process of UOP/Norsk operates for the selective production of ethylene followed by propylene from methanol on a SAPO based catalyst [2, 3]. But achieving high selectivity of propylene is still challenging. The classical representation for the reaction pathways of methanol conversion consist of several consecutive reaction steps initialized by the dehydration of methanol to dimethyl ether (DME) followed by its further dehydration to form light olefins, which are highly reactive to form several hydrocarbon end products such as paraffins, oligomers, aromatics and even the coke precursors responsible for the catalyst deactivation [4]. The key step in effective

Y.-J. Lee (✉) · Y.-W. Kim · K.-W. Jun (✉) · N. Viswanadham · J. W. Bae
Alternative Chemicals/Fuel Research Center, Korea Research Institute of Chemical Technology (KRICT), P.O. Box 107, Daejeon 305-343, Republic of Korea
e-mail: yjlee@krict.re.kr

K.-W. Jun
e-mail: kwjun@krict.re.kr

Y.-W. Kim · H.-S. Park
Department of Chemical and Biomolecular Engineering, Sogang University, C.P.O. Box 1142, Seoul 100-611, Republic of Korea

conversion of methanol to propylene is thus the controlling the reaction at the olefin formation stage or by facilitating the selective cracking of long chain hydrocarbon intermediates to form propylene by adopting an appropriate catalyst with tailored properties to operate at optimized reaction conditions.

Enhanced diffusion of the olefin intermediates in the catalyst also plays a vital role in controlling the secondary reactions. Facilitation of the fast diffusion of the light olefins from the catalyst bed may be advantageous to suppress the formation of otherwise undesired oligomers and aromatics. Recently, attention is given for the development of novel catalysts systems to improve the mechanical strength, diffusion and heat transport properties of the zeolites [7]. Coating of thin layers of zeolite on the ceramic support is generally employed for improving the activity of catalyst and to avoid the pressure drops in the reactor [8–17]. But, this system also suffers from disadvantages such as low zeolite to support ratio, single sided mass transport and leach out of zeolite films with swings of operation conditions due to the differential thermal expansions of the support and the zeolite coatings. Going one step ahead, recent research is focusing on the direct synthesis of rigid, self-supporting zeolite monoliths consist of improved porosity created by the presence of interconnected macro pore network [18–24]. This is generally manifested by virtue of continuous and spontaneous formation of the zeolite crystal film on the surface of templates such as polyurethane foam (PUF) employed during the hydrothermal synthesis of zeolites [25–27]. Such supports are inexpensive and easy to handle to tailor the properties of the zeolite. Earlier we have successfully synthesized monolithic PUF supported silicalite and TS-1 samples exhibiting comparable properties with the corresponding powder samples synthesized by traditional method [26, 27]. The difference in textural properties of such zeolite materials with the traditional ones and their implications on a selected reaction is of prime importance. The present work is aimed to synthesize the ZSM-5 monolith foam (ZMF) samples and explore their catalytic applications. Accordingly, the following aspects of the catalysts have been studied in this work.

1. Synthesis of ZSM-5 foam material with good crystallinity at wide range of framework Si/Al ratios.
2. Catalytic applications of such ZMF materials in methanol conversion as a reaction to see the production of olefins and propylene.
3. Any difference in product selectivity when the foam material is pelletized.

Here we report the successful synthesis of ZMF materials with wide range of framework Si/Al ratios exhibited 100–300 μm range macro pores created by packed growth of orthorhombic shaped ZSM-5 crystals of 5 μm size on the surface of PUF struts and their promising applications as suitable catalysts for the selective production of light olefins especially propylene from methanol at near 100% conversion of methanol. At optimized catalytic properties and reaction conditions, the catalyst exhibited as high as 75% selectivity to $C_2$–$C_4$ olefins with propylene as major component ($\sim$44%).

## 2 Experimental

### 2.1 Synthesis of ZSM-5 Monolith

ZSM-5 monolith foam (ZMF) samples with three different Si/Al ratios of 140, 250 and 500 were synthesized according to our previously established method [25, 26]. The molar gel composition used for the synthesis of ZSM-5 foam with Si/Al = 140 is 7.5 TEOS: 1.0 TPAOH: 0.054 aluminum isopropoxide: 330 $H_2O$. In a typically procedure, aluminum isopropoxide (0.23 g) was first hydrolyzed in a solution consists of 19.3 mL of tetrapropylammonium hydroxide (TPAOH, TCI, 20–25%) and 101.0 mL of $H_2O$ followed by addition of 33.9 g of tetraethyl orthosilicate (TEOS, Acros, 98%). The final gel was stirred for 4 h and transferred to an autoclave containing the 2.5 g of cylindrically shaped polyurethane foam (PUF) template. The air inside the PUF template was removed by frequently squeezing the template with a glass rod during introduction of the gel. The typical volumes of the gel and PUF were 168 mL and 155 $cm^3$, respectively. The hydrothermal synthesis was conducted at 170 °C for 2 days and the as synthesized material (ZSM-5 monolith) was successfully washed with copious amounts of water and acetone followed by its drying at room temperature and calcinations at 600 °C for 12 h under air flow. The calcined ZMF sample (8.5 g) was ion exchanged twice with a 500 mL of 2 M $NH_4NO_3$ solution at 70 °C for 12 h. Then the sample was washed, dried, and calcined to get H-form at 400 °C for 5 h.

The synthesis procedure for the PUF template used in ZMF preparation has been described in our previous paper [25].

### 2.2 Characterization of the Catalysts

The XRD patterns of the synthesized samples were recorded on Rigaku D/MAX IIIB X-ray diffractometer with Cu Kα radiations. The morphology of the ZMF catalyst was observed with scanning electron microscope (Philips XL 30S FEG microscope). The surface acidity of the samples were conducted by temperature programmed desorption of

ammonia ($NH_3$-TPD) using a BEL-CAT PCI 3135 with TCD detector. In a typical analysis, 0.2 g of the calcined sample was pretreated to remove adsorbed water at 500 °C for 3 h and then saturated with ammonia at 100 °C for 1 h. After saturation, the sample was purged with helium for 30 min to remove the weakly adsorbed ammonia on the surface of the catalyst. The temperature of the sample was then raised at a heating rate of 10 °C/min from 100 to 700 °C. The amount of ammonia desorbed from the catalyst was measured by comparing peak areas of standard sample.

BET surface area and pore volumes were measured by $N_2$ adsorption-desorption isotherm at −196 °C using TriStar 3000 (Micromeritics). Prior to the adsorption-desorption measurements, all the samples were degassed at 300 °C in vacuum for 4 h. The compositions of the catalysts were obtained by X-ray fluorescence (XRF) analyses conducted on a SEA 5120 (Seiko Instruments Inc.).

### 2.3 Catalytic Activity

Catalytic activity of all the samples towards methanol conversion was carried out in a fixed bed micro-reactor (316 stainless steel tubing, I.D. = 1 cm and length = 30 cm) at atmospheric pressure in the temperature range of 300–550 °C. ZMF catalyst was cut to 1–2 mm size and loaded into the reactor. For comparison purpose, pelletized ZMF catalyst was prepared by grinding the ZMF to powder followed by its pelletization and sieving into 0.8–1.15 mm size particles. The pelletized catalyst was loaded with sea sand as a diluent in same volume of 2.5 mL with the foam form catalyst in the reactor. In a typical experiment, prior to the activity evaluation, the catalysts were activated for 1 h at 500 °C in a $N_2$ flow prior. Nitrogen gas as an inert diluent was co-fed with crude methanol containing 20 mol% $H_2O$ at a flow-rate of 130 mL/min (MeOH:$N_2$ = 1:9 v/v) and the reaction was carried out under WHSV = 2.55 $h^{-1}$. Effluent gas from the reactor was analyzed by an online gas chromatograph (Donam GC 6100) employing GS-Q capillary columns for hydrocarbons and oxygenates, respectively, with FID detection. Product compositions were calculated based on standard gas mixture. The methanol conversion and product selectivity were calculated according to the following equations:

$$\text{Conversion } (\%) = \frac{(\text{moles of MeOH introduced}) - (\text{moles of MeOH unreacted})}{(\text{moles of MeOH introduced})} \quad (1)$$

$$\text{Hydrocarbon selectivity } (\text{mol}\%\ \text{C}) = \frac{(\text{moles of C in specific hydrocarbon produced})}{(\text{moles of C in total hydrocarbon produced})} \quad (2)$$

## 3 Results and Discussions

### 3.1 Morphology and Textural Properties of ZSM-5 Monolith Foam (ZMF)

The photographs of polyurethane foam (PUF) (Fig. 1a) template and ZMF (Fig. 1b) have shown in Fig. 1. The photographs reveal identical appearance of ZMF with the PUF template (Fig. 1a) in shape and size. The ZMF structure does not shrink even after the calcinations at 550 °C indicating the formation of fully-grown monolith. The cylindrical macro structure of zeolite foam (Fig. 1b) has cut and analyzed for its topology. The SEM analysis of the sample indicated the formation of ZSM-5 monolith exhibiting about 100–300 μm range macro pores (Fig. 1c) created by packed growth of 5 μm size orthorhombic shaped ZSM-5 crystals on surface of PUF struts (Fig. 1d). XRF analysis indicated the Si/Al ratio of 153, 223 and 433 for the three ZMF samples synthesized.

X-ray diffraction patterns of all the ZMF samples exhibited the fundamental band patterns confirming the MFI structure of ZSM-5 (Fig. 2). The intensity of lower degree peaks (below 10°) is increased with the framework Si/Al ratio due to decreased amount of adsorbed water with increased hydrophobic nature of the high silica sample. The samples also exhibited similar type of isotherms in $N_2$ sorption measurements, except a slight increase in pore volume with Si/Al ratio (Fig. 3). Though, the increase in particle size is expected with the Si/Al ratio, there is not much difference in properties viz. surface area and porosity was observed, indicating minimal differences in the particle size of the ZMF with the variation in framework composition. Overall, the ZMF samples exhibited the comparable values of surface area (410 $m^2/g$) and pore volume (0.2 cc/g) (Table 1).

The ZMF sample also exhibited two peak acidity patterns in $NH_3$-TPD and the acidity is decreased with the increasing framework Si/Al ratio of the gel (Fig. 4). The sample ZMF1 has shown a low temperature desorption peak at about 170 °C with a high temperature peak at 380 °C correspond to weak and strong acidity, respectively. The intensity of both the peaks decreased with the Si/Al ratio indicating the decrease in total acidity of the samples with the decrease in aluminum content.

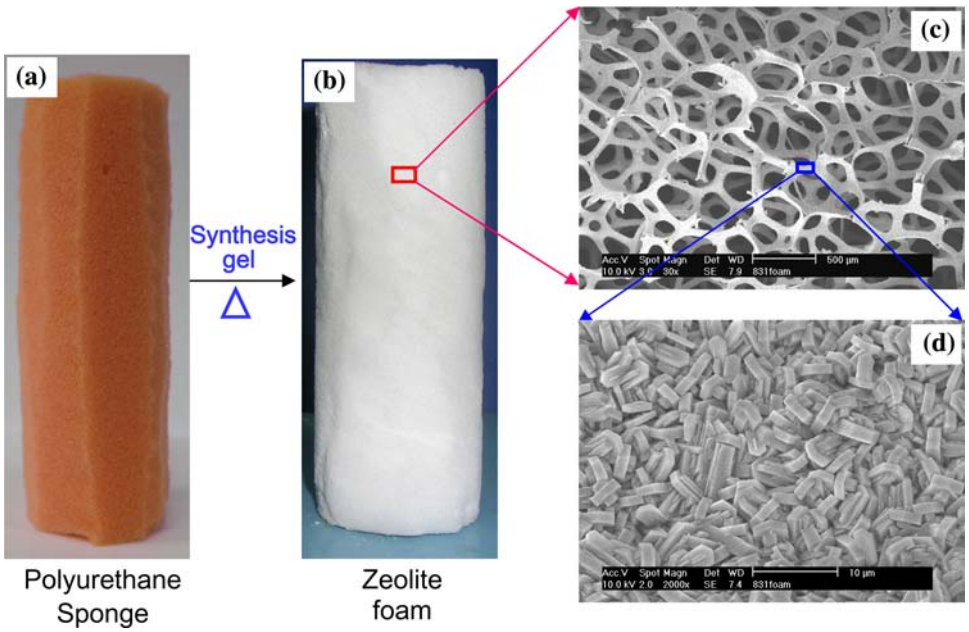


**Fig. 1** Morphology and structure analysis of ZSM-5 monolith foam (ZMF), **a** photograph of polyurethane foam and **b** ZSM-5 monolith foam, **c** SEM images of ZSM-5 foam and **d** magnified portion of ZSM-5 foam

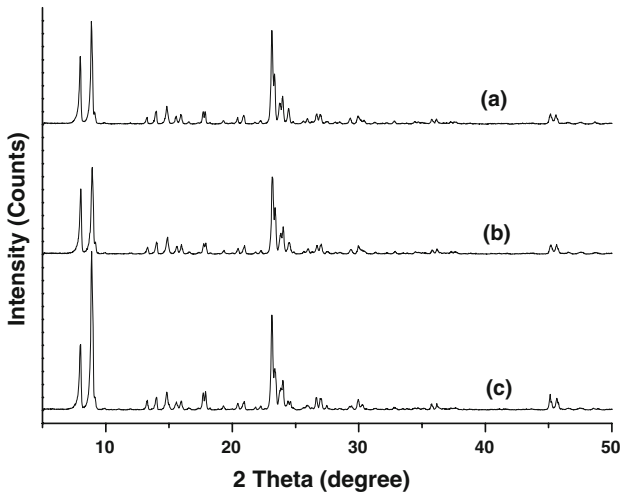


**Fig. 2** X-ray diffraction patterns of the ZMF samples, (a) ZMF1 (Si/Al = 140), (b) ZMF2 (Si/Al = 250), (c) ZMF3 (Si/Al = 500)

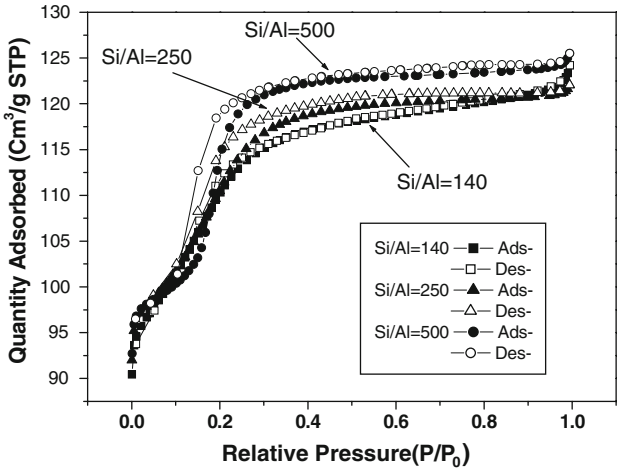


**Fig. 3** Nitrogen adsorption–desorption isotherms of ZMF samples

### 3.2 Catalyst Performance in Methanol Conversion

The product obtained in methanol conversion over three ZMF catalysts at various reaction temperatures has been given in Tables 2, 3, 4. The products obtained are indicated with carbon number of hydrocarbons. Emphasis is given to maximize the formation of $C_2$–$C_4$ olefins with special reference to propylene and $C_3^=/C_3$ ratio.

The ZMF1 (Si/Al = 140) sample exhibited the light olefin selectivity of about 58% at 400 °C and the selectivity is increased with reaction temperature and reached 72% at 550 °C. The main reason for increase in $C_2$–$C_4^=$ at 550 °C is due to the enhanced cracking reactions prevailed at higher reaction temperatures. Decrease in $C_5^+$ hydrocarbon selectivity indeed supports the occurrence of cracking reactions at higher temperatures. Thus, the selectivity to $C_1$–$C_2$ is also increased with reaction temperature. The conversion of methanol is always 100% at all the reaction

**Table 1** Properties of ZSM-5 monolith foam (ZMF) catalysts

| Sample | Si/Al ratio | BET surface area ($m^2/g$)[a] | Total pore volume ($cm^3/g$) |
|---|---|---|---|
| ZMF1 | 140 | 408.4 | 0.192 |
| ZMF2 | 250 | 414.3 | 0.189 |
| ZMF3 | 500 | 416.2 | 0.194 |

[a] Measured by $N_2$ adsorption at −196 °C

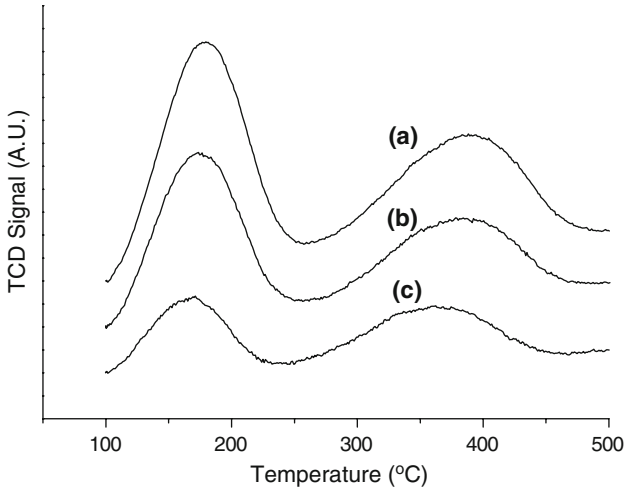


**Fig. 4** $NH_3$-TPD of the ZMF samples, (a) ZMF1 (Si/Al = 140), (b) ZMF2 (Si/Al = 250), (c) ZMF3 (Si/Al = 500)

temperatures and no DME formation was observed in the reaction product of this catalyst. Interestingly, the olefin to paraffin ratio of $C_3$ is increased with the reaction temperature. Overall, rising of reaction temperature caused significant increase in $C_3^=$ selectivity and moderate increase in $C_2^=$ selectivity with simultaneous decrease in selectivity of $C_4^=$ and $C_5^+$ hydrocarbons. Increase in reaction temperature caused increased in selectivity of $C_2$–$C_4^=$, especially $C_3^=$.

Unlike ZMF1, ZMF2 (Si/Al = 250) exhibited higher $C_2$–$C_4^=$ selectivity of about 73% even at lower reaction temperature (400 °C) and the selectivity is not much improved with the reaction temperature (Table 3). Even at 500 °C, the catalyst exhibited only 75% selectivity to $C_2$–$C_4^=$. There is no considerable change in $C_1$–$C_2$ and $C_5^+$ selectivity on this catalyst with the reaction temperature. But, the increased olefinicity of the $C_3$ hydrocarbon was observed with the reaction temperature.

ZMF3 (Si/Al = 500) exhibited rather a different product pattern with lower methanol conversions at lower reaction temperature and the conversion is increased from 83% to 97% with the reaction temperature (Table 4). Surprisingly, about 31% selectivity to DME was observed on this catalyst at 400 °C, which is decreased with reaction temperature and it was only 4.3% at 550 °C. Accordingly, the selectivity to $C_2$–$C_4^=$ is increased with reaction temperature, being 52% at 400 °C to 74% at 550 °C. This trend reveals the shifting of product pattern from DME to light olefins with increasing conversion accomplished by the raise in reaction temperature. The increase in olefinicity of the $C_3$ hydrocarbon ($C_3^=/C_3$ ratio) was also observed in this case, but the increase is much significant on this catalyst up to 500 °C.

It is interesting to see that the formation of light olefins is favored on all the ZMF samples. The formation of light paraffins and oligomerized products ($C_5^+$ hydrocarbons) are low on these catalysts. This may be due to the improved diffusion of reaction intermediates facilitated by the presence of macro pores in the ZMF sample. The well-known methanol conversion consists of the consecutive reaction steps of methanol dehydration to form DME and the equilibrium mixture of methanol and DME undergoes further dehydration to produce light olefins. The appearance of DME and unconverted methanol in the sample

**Table 2** Product distribution in methanol conversion over ZMF1[a]

| Temp. (°C) | MeOH conv. (%) | Product distribution (%) | | | | | | | | | | |
|---|---|---|---|---|---|---|---|---|---|---|---|---|
| | | $C_1$ | $C_2^=$ | $C_2^-$ | $C_3^=$ | $C_3^-$ | $C_4^-$ | $C_4^=$ | $C_2^=$–$C_4^=$ | $C_5^+$ | $C_3^=/C_3^-$ | $C_3^=/C_2^=$ |
| 400 | 100 | 0.4 | 12.0 | 0.1 | 23.6 | 4.5 | 8.8 | 22.0 | 57.7 | 28.6 | 5.2 | 2.0 |
| 450 | 100 | 0.5 | 11.0 | 0.2 | 28.6 | 3.8 | 5.2 | 19.5 | 59.2 | 31.2 | 7.5 | 2.6 |
| 500 | 100 | 1.2 | 16.2 | 0.3 | 35.5 | 3.5 | 3.1 | 18.6 | 69.4 | 21.6 | 10.1 | 2.2 |
| 550 | 100 | 3.2 | 20.9 | 0.5 | 36.3 | 3.0 | 2.3 | 14.4 | 71.6 | 19.4 | 12.1 | 1.7 |

[a] Reaction conditions: feed = $MeOH/H_2O/N_2$ = 1/0.25/11 (molar ratio), WHSV(MeOH) = 2.55 $h^{-1}$

**Table 3** Product distribution in methanol conversion over ZMF2

| Temp. (°C) | MeOH conv. (%) | Product distribution (%) | | | | | | | | | | |
|---|---|---|---|---|---|---|---|---|---|---|---|---|
| | | $C_1$ | $C_2^=$ | $C_2^-$ | $C_3^=$ | $C_3^-$ | $C_4^-$ | $C_4^=$ | $C_2^=$–$C_4^=$ | $C_5^+$ | $C_3^=/C_3^-$ | $C_3^=/C_2^=$ |
| 400 | 100 | 0.4 | 13.5 | 0.0 | 39.0 | 2.1 | 9.3 | 20.3 | 72.8 | 15.0 | 18.6 | 2.9 |
| 450 | 100 | 0.7 | 11.4 | 0.0 | 43.9 | 1.9 | 5.7 | 20.1 | 75.4 | 16.3 | 23.1 | 3.9 |
| 500 | 100 | 1.7 | 12.4 | 0.1 | 43.7 | 1.7 | 4.4 | 19.2 | 75.3 | 16.9 | 25.7 | 3.5 |
| 550 | 100 | 3.0 | 18.0 | 0.3 | 42.9 | 2.0 | 3.4 | 17.8 | 78.7 | 12.6 | 21.5 | 2.4 |

[a] Reaction conditions: feed = $MeOH/H_2O/N_2$ = 1/0.25/11 (molar ratio), WHSV(MeOH) = 2.55 $h^{-1}$

**Table 4** Product distribution in methanol conversion over ZMF3

| Temp. (°C) | MeOH conv. (%) | Product distribution (%) | | | | | | | | | | | |
|---|---|---|---|---|---|---|---|---|---|---|---|---|---|
| | | $C_1$ | $C_2^=$ | $C_2^-$ | $C_3^=$ | $C_3^-$ | DME | $C_4^-$ | $C_4^=$ | $C_2^=$–$C_4^=$ | $C_5^+$ | $C_3^=/C_3^-$ | $C_3^=/C_2^=$ |
| 400 | 83.0 | 0.4 | 6.6 | 0.0 | 30.7 | 0.4 | 30.8 | 6.1 | 14.1 | 51.6 | 10.8 | 76.8 | 4.7 |
| 450 | 90.8 | 0.6 | 5.4 | 0.0 | 39.6 | 0.2 | 15.3 | 5.0 | 20.2 | 65.0 | 13.8 | 198.0 | 7.3 |
| 500 | 94.8 | 1.1 | 6.8 | 0.0 | 42.4 | 0.2 | 8.1 | 3.9 | 21.7 | 71.0 | 15.8 | 212.0 | 6.2 |
| 550 | 97.2 | 2.6 | 9.5 | 0.1 | 41.7 | 0.5 | 4.3 | 2.7 | 22.8 | 74.4 | 15.8 | 83.4 | 4.4 |

[a] Reaction conditions: feed = $MeOH/H_2O/N_2$ = 1/0.25/11 (molar ratio), WHSV(MeOH) = 2.55 $h^{-1}$

ZMF3 may be due to its lower catalytic activity caused by high framework Si/Al ratio and lower acidity values. On the other hand, the strong acidity in ZMF1 may be responsible for the formation of high $C_1$–$C_2$ hydrocarbons along with the light olefins ($C_2$–$C_4^=$). In case of ZMF2, the optimum acidity seems to be responsible for the formation of high amount of light olefins. Overall, there is an optimum catalytic property that is required for the production of light olefins over the ZMF catalyst. Presence of strong acidity and high reaction temperatures on ZMF1 encouraged secondary reactions to form light paraffins and oligomerized $C_5^+$ hydrocarbons. On the other hand, the ZMF2 could give high amount of light olefins at lower reaction temperatures and the higher reaction temperatures caused the formation of secondary reaction products. On ZMF3, the lower reaction temperatures caused relatively low methanol conversion and the formation of DME (intermediate species of light olefin formation), and increase in reaction temperature caused the decrease of DME with simultaneous formation of light olefins. All these results suggest the importance of catalyst acidity and reaction temperatures on the product selectivity that can be described in the reaction pathways shown below.

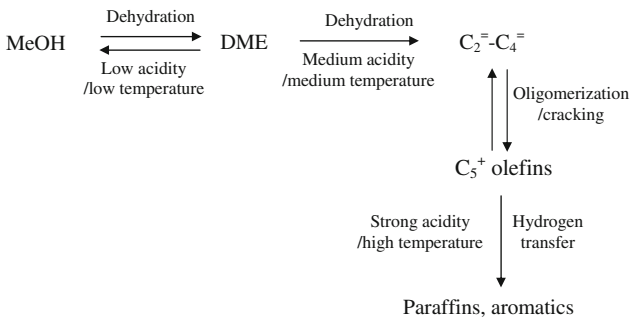


High acidity is good for light olefin formation, but this also encourages secondary cracking reactions to produce ethylene. Decrease of strong acidity is advantageous for propylene production. Indeed the trend observed from ZMF1 to ZMF3 is the increase in $C_3^=/C_2^=$ ratio which is advantageous for the production of propylene with controlled formation of ethylene.

### 3.3 Performance of Pelletized ZMF

Among the three foam samples, ZMF-2 has exhibited the best yields of light olefins and propylene selectivity. Hence, this sample has been considered for further study to understand the role of porosity created in the foam catalyst on the product selectivity. For this, the ZMF2 sample is crushed to the powder and pelletized (ZMF-2P) and the catalytic activity of ZMF-2P is compared with that of the ZMF2. Purpose of this study is to understand the role of macro pores created in ZMF on the reaction. The ZMF-2P also exhibited the typical product pattern of light olefins and the phenomenon of increased light olefin formation with reaction temperature (Table 5). However, the product selectivity of light olefins on the ZMF-2P is not as high as that on the ZMF2. As shown in Table 5, pelletization caused decrease in light olefins with simultaneous increase of $C_5^+$ selectivity at all the reaction temperatures. This may be due to the decrease in free diffusion of the olefinic intermediates in the pelletized sample.

In order to understand the relative selectivities of the hydrocarbon products on the both the catalysts, the product obtained at various reaction temperatures has been compared in Fig. 5. The light olefins, especially propylene selectivity is lower on the pelletized catalyst. However, the pelletization could increase the formation of $C_5^+$ hydrocarbons. This again reveals the better performance of foam catalyst before pelletization due to the presence of macro pores in it. The methanol conversion is near 100% at all these conditions.

Further studies are conducted to understand the performances of these catalysts at lower methanol conversions, where, the foam (ZMF2) and pelletized catalysts (ZMF-2P) have been studied at lower reaction temperature (350 °C) by varying feed flow rate from 1 to 15 WHSV range. The product trends given in Fig. 6 clearly suggest the inferiority of the pelletized catalyst at all the space velocities. The ZMF2 exhibited better selectivity in terms of light olefins, whereas, methanol and DME are relatively low. It is interesting to see that the difference in product pattern is much significant at the higher WHSV values. That means,

**Table 5** Product distribution in methanol conversion over pelletized foam catalyst (ZMF-2P)

| Temp. (°C) | MeOH conv. (%) | Product distribution (%) | | | | | | | | | | |
|---|---|---|---|---|---|---|---|---|---|---|---|---|
| | | $C_1$ | $C_2^=$ | $C_2^-$ | $C_3^=$ | $C_3^-$ | $C_4^-$ | $C_4^=$ | $C_2^=$–$C_4^=$ | $C_5^+$ | $C_3^=/C_3^-$ | $C_3^=/C_2^=$ |
| 400 | 100 | 0.4 | 9.8 | 0.1 | 35.4 | 1.7 | 5.9 | 22.9 | 68.1 | 23.9 | 20.8 | 3.6 |
| 450 | 100 | 0.6 | 10.4 | 0.1 | 41.5 | 1.8 | 4.3 | 20.8 | 72.7 | 20.5 | 23.1 | 4.0 |
| 500 | 100 | 2.1 | 12.8 | 0.2 | 43.8 | 1.7 | 3.1 | 17.9 | 74.5 | 18.7 | 25.8 | 3.4 |
| 550 | 100 | 3.6 | 19.5 | 0.3 | 43.3 | 1.9 | 2.6 | 16.2 | 79.0 | 12.6 | 22.8 | 2.2 |

[a] Reaction conditions: feed = $MeOH/H_2O/N_2$ = 1/0.25/11 (molar ratio), WHSV(MeOH) = 2.55 $h^{-1}$

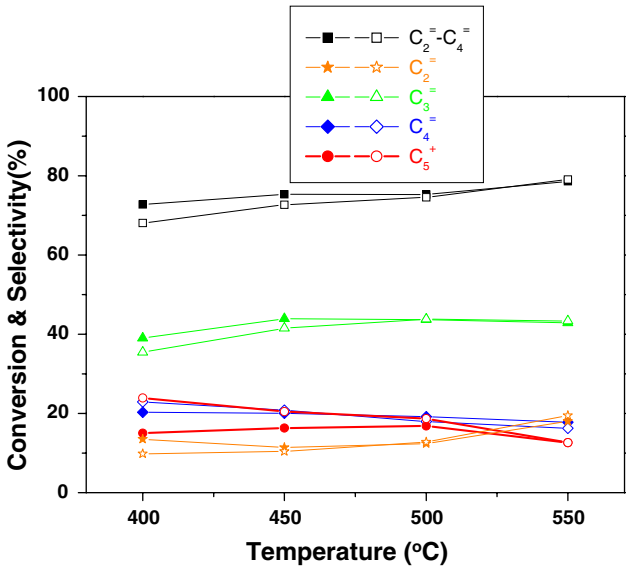


**Fig. 5** Effect of pelletization of the foam on the product distribution in methanol conversion, *filled symbols* (foam), *open symbols* (pellet). Reaction conditions: feed = $MeOH/H_2O/N_2$ = 1/0.25/11 (molar ratio), WHSV (MeOH) = 2.55 $h^{-1}$

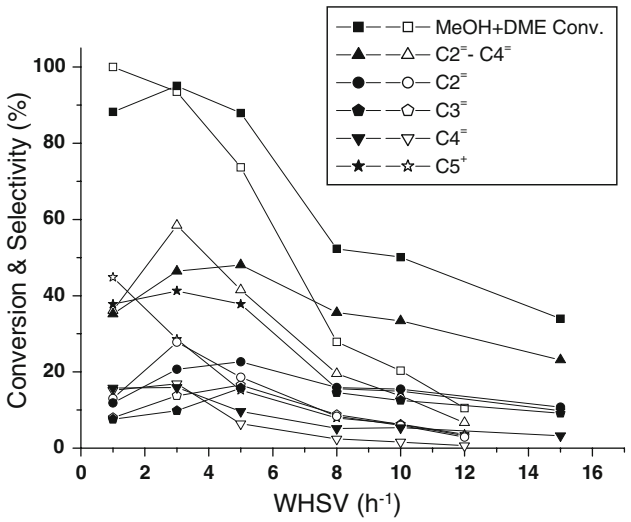


**Fig. 6** Effect of WHSV on the performance of foam (ZMF2) and pelletized foam (ZMF-2P) catalysts in methanol conversion, *filled symbols* (foam), *open symbols* (pellet), Reaction temperature = 350 °C

at higher feed flow rates, the absence of macro pores in pelletized catalyst can decrease the molecular diffusion to yield less light olefins. These results clearly reveal the positive role of macro pores in foam catalyst on the product pattern perhaps through its effective diffusion of the reaction intermediates and products.

Overall, the studies reveal the promising catalytic activity of ZSM-5 monolith foam (ZMF) materials for the conversion of methanol to produce light olefins, where, the catalyst acidity and reaction temperature play a vital role in determining the product selectivity.

## 4 Conclusions

1. ZSM-5 monolith foam (ZMF) materials with various Si/Al ratios can be successfully synthesized in the laboratory.
2. The materials find interesting catalytic applications in methanol conversion and the ZMF exhibits higher selectivity to light olefins, especially propylene in methanol conversion.
3. The ZMF catalyst with high macro porosity exhibited superior catalytic activity compared to its pelletized form signifies the importance of macro porous structure of ZMF in facilitating the enhanced mass transport for the labile diffusion of light olefins.

**Acknowledgments** The authors would like to acknowledge funding from the Korea Ministry of Knowledge Economy (MKE) through ''Project of next-generation novel technology development'' of ITEP. Dr. N. Viswanadham is thankful to Korea Federation of Science & Technology (KOSEF) for giving Brain-Pool fellowship.

## References

1. Brogen M, Svelle S, Joensen F, Nerlov J, Kolboe S, Bonino F, Palumbo L, Bordiga S, Olsbye U (2007) J Catal 249:195
2. Keil FJ (1999) Micropor Mesopor Mater 339:36
3. Chen JQ, Bozzano A, Glover B, Fuglerud T, Kvisle S (2005) Catal Today 106:103

4. Stocker M (1999) Micropor Mesopor Mater 29:3
5. Zhu Q, Hinode M, Yokoi T, Kondo JN, Kubota Y, Tatsumi T (2008) Micropor Mesopor Mater 116:253
6. Cui Z-M, Liu Q, Ma Z, Bian S-W, Song W-G (2008) J Catal 258:83
7. Patcas FC (2005) J Catal 231:194
8. Shan Z, van Kooten WEJ, Oudshoorn OL, Jansen JC, van Bekkum H, van den Bleek CM, Calis HPA (2000) Micropor Mesopor Mater 34:81
9. Davis SP, Borgstedt EVR, Suib SL (1990) Chem Mater 2:712
10. Boudreau LC, Kuck JA, Tsapatsis M, Membr J (1999) Science 152:41
11. Hedlund J, Noack M, Kölsch P, Creaser D, Caro J, Sterte J (1999) J Membr Sci 159:263
12. Bein T (1996) Chem Mater 8:1636
13. Caro J, Noack M, Kölsch P, Schäfer R (2000) Micropor Mesopor Mater 38:3
14. Kormarneni S, Katsuki H, Furuta SJ (1998) Mater Chem 8:2327
15. Zampieri A, Colombo P, Mabande GTP, Selvam T, Schwieger W (2004) Adv Mater 16:819
16. Wine G, Tessonnier J-P, Rigolet S, Marichal C, Ledoux M-J, Huu C-P (2006) J Mol Catal A 248:113
17. Seijger GBF, Oudshoorn OL, van Kooten WEJ, Jansen JC, van Bekkum H, van den Bllek CM, Calis HPA (2000) Micropor Mesopor Mater 39:195
18. Anderson MW, Holmes SM, Hanif N, Cundy CS (2000) Angew Chem Int Ed 39:2707
19. Zhang B, Davis SA, Mendelson NH, Mann S (2000) Chem Commun 781
20. Holland BT, Abrams L, Stein A (1999) J Am Chem Soc 121:4308
21. Tosheva L, Valtchev V, Sterte J (2000) Micropor Mesopor Mater 35–36:621
22. Valtchev V, Schoeman BJ, Hedlund J, Mintova S, Sterte J (1996) Zeolites 17:408
23. Ha K, Lee Y-J, Jung D-Y, Lee JH, Yoon KB (2000) Adv Mater 12:1614
24. Huang L, Wang Z, Sun J, Miao L, Li Q, Yan Y, Zhao D (2000) J Am Chem Soc 122:3530
25. Lee YJ, Lee JS, Park YS, Yoon KB (2001) Adv Mater 13:1259
26. Lee YJ, Yoon KB (2006) Micropor Mesopor Mater 88:176
27. Kim WJ, Kim TJ, Ahn WS, Lee YJ, Yoon KB (2003) Catal Lett 91:123